Available online at www.sciencedirect.com

ScienceDirect

Procedia Structural Integrity 6 (2017) 40–47

Structural Integrity Procedia

www.elsevier.com/locate/procedia

XXVII International Conference "Mathematical and Computer Simulations in Mechanics of Solids and Structures". Fundamentals of Static and Dynamic Fracture (MCM 2017)

Ballistic Characteristics of Bi-layered Armour with Various Aluminium Backing against Ogive Nose Projectile

J. Venkatesan[a,*], M. A. Iqbal[a], N. K. Gupta[b], V. Bratov[c], N. Kazarinov[c], F. Morozov[c]

[a]*Department of Civil Engineering, Indian Instiute of Technology Roorkee, Roorkee 247667, India*
[b]*Department of Applied Mechanics, Indian Institute of Technology Delhi, New Delhi 110016, India*
[c]*Institute for problems in Mechanical Engineering of the Russian Academy of Sciences, Saint Petersburg State University, St.Petersburg, Russia*

Abstract

The present study focused the effect of aluminium series backing layer on the ballistic resistance of bi-layer ceramic/metal target by means of three dimensional numerical simulation using ANSYS/AUTODYN explicit solver which is cable of modeling and solving the 3D explicit problems. The ceramic and metal layer of bi-layer target was alumina 95% and 1100-H12, 2024-T3, 6061, 7075 aluminium respectively and the impact velocity of ogive nose projectile of 4340 steel was 493, 820 and 1200 m/s. The strength and failure mode of alumina, and steel and aluminium under the projectile impact was computationally modelled by Johnson-Holmiquist (JH-2) model and Johnson-Cook (JC) model respectively. The results shows that ballistic resistance of bi-layer target significantly varied with the aluminium series. 7075 aluminium backing helped the bi-layer target to offer high resistance to the projectile penetration for all the impact velocities.

Keywords: Type your keywords here, separated by semicolons ;

1. Introduction

Metals have been an armour for a several decades. However, it is not effective for mobility due to its high density which necessitated search of alternative material for armour application with low density and other required properties

* Corresponding author. Tel.: +0-000-000-0000 ; fax: +0-000-000-0000 .
E-mail address: jsvenkat.c@gmail.com

2452-3216 Copyright © 2017 The Authors. Published by Elsevier B.V.
Peer-review under responsibility of the MCM 2017 organizers.
10.1016/j.prostr.2017.11.007

of armour. Ceramic becomes substitute to the metal armour due to its low density, high hardness and compressive strength. Nevertheless, its low tensile strength and toughness has not allowed them to be used as a monolithic layer for armour application instead it is used with metals or fiber composite materials as a backing layer.

Ceramic materials such as alumina, silicon carbide, boron carbide are the most commonly used ceramic layer and aluminium, armour steel, composite fibers of aramid fibers (Kevlar, Twaron), polyethylene fibers and polypropylene fibers are the backing layer of the armour. Bi-layer ceramic/metal armour contains front layer of ceramic and back layer of metal. The function of ceramic is to damage and erode the projectile and the metal backing layer is to keep the fractured ceramic material in place and dissipate the part of projectile kinetic energy through ductile failure. The ballistic resistance of this armour system is depends on several factors such as geometry and arrangement of target plates, physical and mechanical properties of projectile and target material, and projectile impact velocity and angle of impact [1]. It would be very expensive to study all these parameters through experimentally. Therefore, numerical simulation is a way to study the effect of these parameters on the ballistic resistance of bi-layer ceramic/metal targets and deep understanding of penetration mechanism and failure of the projectile and target.

Mayseless et al. (1987) conducted ballistic experiments to study the effect of projectile incident velocity on alumina/aluminium alloy 2024-0, 6061-T6 and alumina/steel 1010, 4130 targets. The results showed that the bi-layer target ballistic resistance was lower at low incident velocity, 250 ms^{-1} and higher as the incidence velocity increased. The erosion of projectile was depends on the incidence velocity of projectile and the thickness of ceramic layer. Hetherington (1992) tested alumina/aluminium alloy 5083 with various thicknesses against 7.62 mm AP projectile to determine the optimum thickness ratio of alumina and aluminium layers for the given areal density and a simple numerical relationship also developed to calculate the thickness of layers. The optimum thickness ratio of alumina/aluminium was found to be 2.5. The similar study was conducted by Lee and Yoo (2001) using ballistic experiments and 2D numerical simulations. The failure mode of the target was changed with the change in the thickness of ceramic and aluminium layer and the reported optimum thickness ratio was also 2.5. Serjouei et al. (2015) optimised the alumina/aluminium 2024-T3 target thickness ratio using experimental and numerical simulation. The optimum thickness ratio of target was 0.5 to 0.6 which is different from the above reported optimum thickness ratio. Sadanandan and Hetherington [6] studied the effect of oblique incidence of projectile on the ballistic limit of alumina/steel 43A and alumina/aluminium alloy 5083. Ballistic limit of the target increased with the oblique angle and it was due the higher areal density of the target. Goncalves et al. (2003) developed a one dimensional analytical model to predicting the ballistic resistance of ceramic/metal armour against projectile impact and also experiments were carried out to validate the analytical model and study the grain size effect on the ballistic resistance of alumina. The thickness and hardness of ceramic layer played a major role to dissipate the kinetic energy of the projectile.

The effect of projectile nose shape on the ballistic resistance of bi-layer ceramic/metal target was studied by Venkatesan et al. (2017). The projectile nose shape considerably affected the ballistic resistance of the target. Gour et al. (2017) studied the ballistic resistance of bi-layer target with various hardness of weldox steel backing layer through numerical simulation. It was observed that the ballistic resistance of bi-layer target significantly improved by the steel with high hardness. It could been seen from the above studies that the optimisation of bi-layer ceramic/metal target was the major interest and in the most of the studies, aluminium alloy was the metal backing as it offers lower weight than the steel. As it was reported in Gour et al. (2017), the variation steel backing significantly affected the ballistic resistance of bi-layer target. Therefore it could be conceived that the different series of aluminium alloys also affect the ballistic resistance.

In this study, four different aluminium alloys have been used as a backing layer of bi-layer ceramic/metal target to explore its effect on ballistic resistance of bi-layer target using 3D numerical simulation. ANSYS/AUTODYN explicit solver is used for the current numerical simulation. Alumina 95% and aluminium alloys of 1100-H12, 6061, 2024-T3 and 7075 grades have been used as a front and back layer of bi-layer target respectively.

2. 3D Numerical modelling

The current numerical study was carried out using the explicit dynamic solver ANSYS/AUTODYN which is capable of simulating the behaviour of ductile and brittle materials subjected to large deformation, high strain rate, temperature and pressure.

2.1. Projectile

Ogive nose projectile of steel 4340 was used for the current study with the diameter, shank length and ogive nose length of 7.56 mm, 22.98 mm and 7.56 mm respectively. It was modelled as a deformable body and meshed with Lagrangian element of 0.6 mm size see Fig. 1.

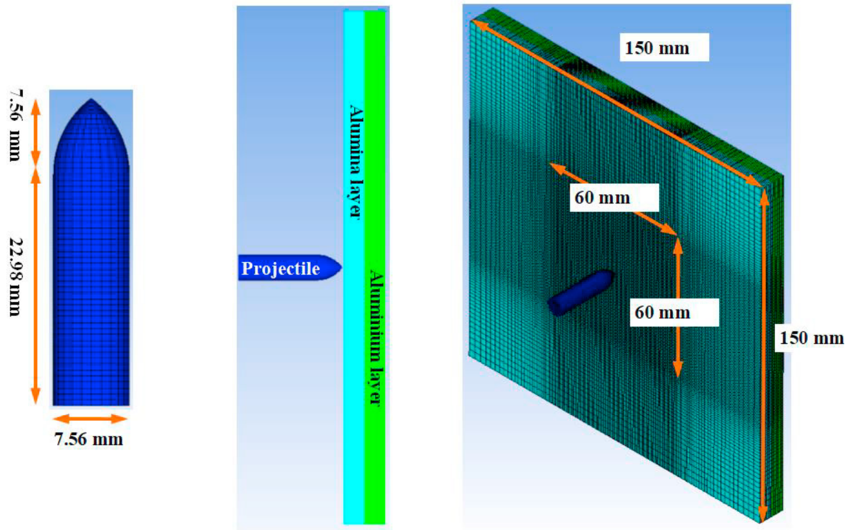

Fig. 1. Dimension and meshing details of projectile and target

Hexahedral elements were used all over the projectile except at the tip of nose which was meshed with prism elements. The incidence angle of projectile to the target was perpendicular. Johnson-Cook (JC) phenomenological constitutive model (strength and failure model) was used to predict the material behaviour of steel 4340 under large strain, high strain rate and temperature. This constitutive model is well described elsewhere Iqbal et al. (2015). The input data to define the constitute behaviour of steel 4340 was taken from the serjouei et al. (2015) study see Table. 1.

Table 1. Johnson-Cook model parameters of steel and different aluminium series

Constants	Units	4340 Steel (serjouei et al. 2015)	Aluminium series			
			1100-H12 (Zaid et al. 2017)	6061-T6 (Manes et al. 2013)	7075-T651 (Jomaa et al. 2017)	2024-T3 (Kay 2002)
Density, ρ_0	g/cm3	7.770	2.7	2.7	2.81	2.785
Bulk modulus, K_1	kPa	159×10^6	5.48×10^7	6.86×10^7	7.029×10^7	–
Gruneisen constant		–	–	–	–	2
Parameter, C_1	m/s	–	–	–	–	5328
Parameter, S_1		–	–	–	–	1.338
Specific heat, C_r	(J/Kg. K)	477	920	890	960	874.9
Shear modulus, G	kPa	77×10^6	2.53×10^7	2.63×10^7	2.695×10^7	2.692×10^7
Static yield strength, A	kPa	9.5×10^5	1.48361×10^5	2.7×10^5	5.27×10^5	1.67×10^5

Strain hardening constant, B	kPa	7.25×10^5	3.45513 $\times 10^5$	1.543×10^5	5.75×10^5	6.84×10^5
Strain hardening exponent, n		0.375	0.183	0.2215	0.72	0.551
Strain rate constant, C		0.015	0.001	0.1301	0.017	0.001
Thermal softening exponent, m		0.625	0.859	1.34	1.61	0.859
Melting temperature, t_m	K	1793	893	925	908	893
Reference strain rate, $\dot{\varepsilon}_0$		1	1	1	1	1
Damage constant, d_1		-0.8	0.071	−0.77	0.11	0.112
Damage constant, d_2		2.1	1.248	1.45	0.572	0.123
Damage constant, d_3		−0.5	−1.142	−0.47	−3.446	1.5
Damage constant, d_4		0.002	0.0097	0.011	0.016	0.007
Damage constant, d_5		0.61	0	1.6	1.099	0

2.2. Target

The bi-layer ceramic/metal consist of alumina as a ceramic layer and different grade of aluminium as a metal layer. Alumina 95% ceramic plate was considered and both the width and breadth of the plate was 150 mm and thickness was 6 mm for all the simulation. The centre zone of 60 mm × 60 mm of ceramic layer was meshed with 0.6 mm hexahedral element and the other portion was meshed with gradual varying size.

The material behaviour was defined by Johnson Holmiquist (JH-2) constitutive model. This model is widely used for computational modelling of ceramics which experiences gradual softening as the material undergoes damage during impulse and impact loading. It defines the strength and failure as a function of pressure and strain rate. The complete description of the model can be found elsewhere Johnson and Holmiquist (1994). The JH-2 material model parameters for alumina 95% is given in the Table.2.

Table 2. JH-2 material model constants for Al2O3 95%

Constants	Units	Al2O3 95% (serjouei et al. 2015)
Density, ρ_0	g/cm3	3.741
Bulk modulus, K_1	kPa	1.8456×10^8
Pressure constant, K_2	kPa	1.8587×10^8
Pressure constant, K_3	kPa	1.5754×10^8
Shear modulus, G	kPa	1.2034×10^8
Hugoniot elastic limit, HEL	kPa	6×10^6
Intact strength constant, A		0.889
Intact strength exponent, N		0.764
Strain rate constant, C		0.0045
Fracture strength constant, B		0.29
Fracture strength exponent, M		0.53
Normalized maximum fractured strength, σ^*_{Fmax}		1
Normalized hydrostatic tensile limit, T^*	kPa	-0.3×10^6
Damage constant, d_1		0.005
Damage exponent, d_2		1
Bulking factor, β		1

Aluminium alloys of 1100-H12, 6061, 2024-T3 and 7075 grade were used for the current study as a metal layer. The dimension and meshing of these layers are same as ceramic layer. JC strength and failure model was used for defining the constitute behaviour of all the aluminium alloys. The constitute model parameters are listed in Table. 1.

The interaction between the projectile and target was defined by trajectory based contact detection algorithm and the connection of alumina and aluminium layer was established by bond interaction model available in ANSYS/AUTODYN. Geometrical erosion criteria was assigned to all the parts of current simulation to alleviate the element distortion during the large deformation.

3. Results and discussion

3.1. Model validation

The current numerical model validated against the experimental results of serjouei et al. (2015). A bi-layer target of alumina 95%/2024 aluminium was impacted by 4340 steel blunt nose projectile. Three experimental results were validated using 3D finite element model. Table 3 shows the current finite element model prediction and experimental finding of projectile residual velocity. It could be seen that the model is capable of simulating the ballistic response of bi-layer target.

Table 3. Comparison of experimental results serjouei et al. (2015) with the current 3D model simulation results

Impact velocity	Experimental	Simulation	%Error
655	351	332.58	5.25
775	370	389	-5.14
948	605	600.78	0.70

3.2. Effect of aluminium layer

The effect of different series of aluminium backing layer on the ballistic performance of bi-layer target was evaluated by comparing the residual velocity of the projectile. As it was shown in Fig. 2, the residual velocity of projectile was increased with the impact velocity and the increase was second order polynomial trend with irrespective of aluminium series. The variation of residual velocity of projectile was higher at lower impact velocity and it begin to reduce as the impact velocity increased for different aluminium series. It can be concluded that difference in the aluminium series is not affecting the ballistic resistance of bi-layer target significantly when it subjected to high impact velocity.

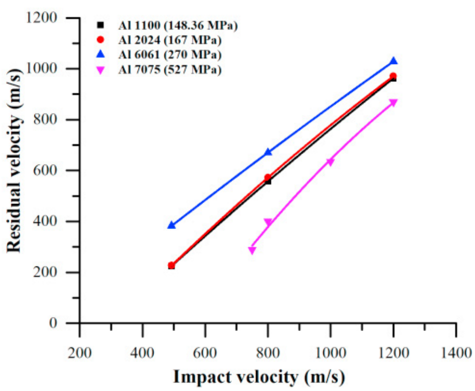

Fig. 2. Variation of projectile residual velocity due to different series of aluminium as metal layer of bi-layer target

Ballistic resistance of bi-layer target with 2024 and 1100 aluminium series as a backing layer was almost same. 7075 aluminium displayed excellent ballistic resistance as compare to other aluminium. It could be due to its higher yield strength. However, 6061 aluminium which had higher yield strength than 2024 and 1100 aluminium was not displayer higher resistance. Therefore, the contribution of aluminium series on ballistic resistance of bi-layer target was not alone depend on its yield strength but also other properties such as strain hardening constants and failure constants of the material Senthil et al. (2017).

3.3. Fracture and failure modes

The fracture and failure of alumina/2024 aluminium and 4340 steel projectile erosion at 493 m/s and 1200 m/s is shown in Fig. 3. The fracture width of alumina layer was increased with the impact velocity of projectile see Fig. 4. However, the damage increased in the later stage of penetration process of projectile at 1200 m/s impact velocity. It attributed ceramic to dissipate much of the projectile kinetic energy through damage and projectile. Nevertheless, the length of damage width of the metal layer was completely opposite to the ceramic layer as the length was larger with higher impact velocity. It might be the cause of fractured ceramic at the front of projectile which moves away at impact velocity of 493 m/s and was not participated during the projectile penetration into metal layer. Whereas, at impact velocity of 1200 m/s, the fractured ceramic was not moved away due to the confining effect experienced from the surrounding material and it participates in the projectile further penetration. The same phenomena was observed in all targets with different aluminium layers. Hence, metal layer target would alone be suitable for low range impact cases than bi-layer ceramic/metal target Mayseless et al. (1987).

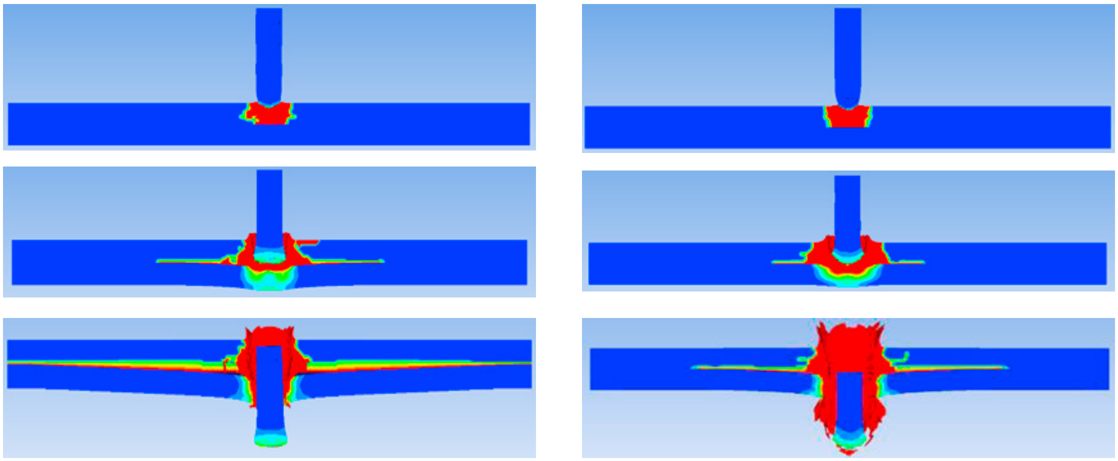

(a) (b)

Fig. 3. Projectile penetration into alumina/1100 aluminium target at impact velocity of (a) 493 m/s; (b) 1200 m/s

The defamation of different series of aluminium layer was compared for 493 m/s and 1200 m/s impact velocities see Fig. 5. The deformation of aluminium layer was decreased irrespective of aluminium series. However, there was difference the deformation among the aluminium series at same impact velocities. 1100 aluminium series displayed higher deformation and 6061 aluminium was not shown any deformation for both the impact velocities. It implies that 1100 aluminium is capable of maintaining its ductility properties even under high strain rate condition. Although the 2024 aluminium was not deformed equal to the 1100 aluminium the ballistic performance was same for both the material Fig. 5.

Fig. 6 compares the residual length of projectile for low and high impact velocity. 4340 steel projectile eroded more at higher impact velocity and it was not sensitive to the aluminium series except 7075 aluminium. Most of the projectile erosion was caused by ceramic layer.

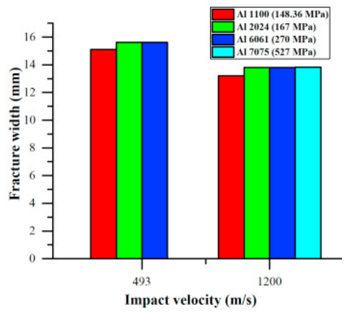

Fig. 4. Alumina fracture width during initial stage of projectile and target interaction

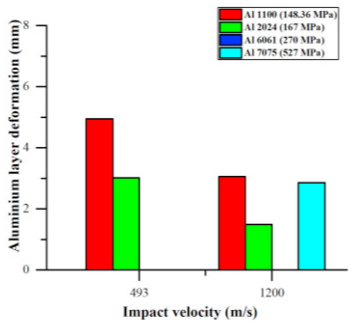

Fig. 5. Deformation of aluminium layer at 493 and 1200 m/s

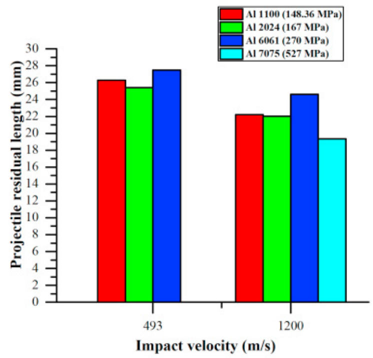

Fig. 6. Effect of impact velocity and aluminium series on projectile erosion

4. Conclusions

The effect of backing metal layer on the ballistic resistance of bi-layer ceramic/metal target was explored through a 3D numerical simulation. The ballistic resistance of the target was significantly affected by the aluminium series. Among the four series of aluminium, 7075 and 6061 aluminium were having higher and poor ballistic resistance respectively. Although the series of 1100 and 2024 aluminium was not having same material properties, both exhibited almost equal ballistic performance. Therefore, the ballistic resistance of bi-layer ceramic/metal target can be improved using appropriate aluminium series as a metal layer. However, bi-layer ceramic/metal target was not shown excellent ballistic resistance at low impact velocities. Hence, it is suggested that the only metal layer would be an effective armour for low impact velocity.

Acknowledgments

Authors gratefully acknowledge the financial support provided by Department of Science and Technology, Government of India through the research grant no. INT/RUS/RFBR/P-232 for carrying out the present study.

References

Espinosa, H. D., Dwivedi, S., Zavattieri, P. D., Yuan, G., 1998. A numerical investigation of penetration in multilayered material/structure systems. International Journal of Solids Structures 35, 2975–3001.

Mayseless, M., Goldsmith W., Virostek, S. P., Finnegan, S. A., 1987. Impact on Ceramic Targets. Journal of Applied Mechanics 54:373.

Hetherington, J. G., 1992. The optimization of two component composite armours. International Journal of Impact Engineering 12:409–414.

Lee, M., Yoo, Y. H., 2001. Analysis of ceramic/metal armour systems. International Journal of Impact Engineering 25:819–829.

Serjouei, A., Chi, R., Zhang, Z., Sridhar, I., 2015. Experimental validation of BLV model on bi-layer ceramic-metal armor. International Journal of Impact Engineering 77:30–41.

Sadanandan, S., Hetherington, J. G., 1997. Characterisation of ceramic/steel and ceramic/aluminium armours subjected to oblique impact. International Journal of Impact Engineering 19, 811–819.

Gonçalves, D. P., de Melo, F. C. L., Klein, A. N., Al-Qureshi, H. A., 2004. Analysis and investigation of ballistic impact on ceramic/metal composite armour. International Journal of Machine Tools and Manufacture 44:307–16.

Venkatesan, J., Iqbal, M. A., Madhu, V., 2017. Ballistic performance of bilayer alumina/aluminium and silicon carbide/aluminium armours. Procedia Engineering 173, 671-678.

Gour, G, Serjouei, A., Sridhar, I., 2017. Influence of Geometry and Hardness of the Backing Plate on Ballistic Performance of Bi-Layer Ceramic Armor. Procedia Engineering 173:93–100.

Iqbal, M. A., Senthil, K., Bhargava, P., Gupta, N. K. , The characterization and ballistic evaluation of mild steel. International Journal of Impact Engineering 78, 98–113.

Mohammad, Z., Gupta, P. K., Iqbal, M. A., Baqi, A., 2017. Energy Absorption in Metallic Targets Subjected to Oblique Impact. Procedia Engineering 173, 145–52.

Manes, A., Lumassi, D., Giudici, L., Giglio, M., 2013. An experimental–numerical investigation on aluminium tubes subjected to ballistic impact with soft core 7.62 ball projectiles. Thin-Walled Structure 73, 68–80.

Jomaa, W., Mechri, O., Lévesque, J., Songmene, V., Bocher, P., Gakwaya, A., 2017. Finite element simulation and analysis of serrated chip formation during high–speed machining of AA7075–T651 alloy. Journal of Manufacturing Processes 26, 446–58.

Kay, G., 2002. Failure modeling of titanium-61-4V and 2024-T3 aluminum with the Johnson-Cook material model. Tech Rep Lawrence Livermore Natl Lab Livermore CA 2002.

Johnson, G. R., Holmquist, T. J., 1994. An improved computational constitutive model for brittle materials. Journal of Applied Physics 309, 981–984.

Senthil, K., Iqbal, M. A., Chandel, P. S., Gupta, N. K. 2017. Study of the constitutive behavior of 7075-T651 aluminum alloy. International Journal of Impact Engineering 108, 171-190.